Available online at www.sciencedirect.com
SCIENCE DIRECT®
Journal of Sound and Vibration 260 (2003) 549–564
JOURNAL OF SOUND AND VIBRATION
www.elsevier.com/locate/jsvi

Letter to the Editor

Added mass and damping of submerged perforated plates

Jyoti K. Sinha*, Sandeep Singh, A. Rama Rao

Vibration Laboratory, Reactor Engineering Division, Bhabha Atomic Research Centre, Mumbai-400 085, India

Received 11 December 2001; accepted 19 June 2002

1. Introduction

It is well known that structural component, when submerged in fluid exhibit decrease in natural frequencies and increase in damping. In general, the surrounding fluid exerts a reaction force on the structure which is represented as an added mass and a damping contribution to the dynamic response of the component without affecting its structural stiffness. These dynamic parameters for the submerged structures can be obtained by conducting modal test [1]. However, at design stage such a modal test may not be possible. Hence, a fairly accurate quantification of added mass and damping is important for a good estimation of the response of these submerged structures.

Many studies have been reported in the literature for the estimation of these parameters for many commonly used geometrical shapes. A review of study on these dynamic parameters for different configurations of array of tubes/cylinders has been made by Chen [2] and wide range of objects with different shapes of cross-section and structural configurations has been briefly reviewed by Blevins [3,4] and Naudascher and Donald [5]. Recently, Sinha and Moorthy [6] has also given the formulation for added mass for the submerged perforated tubes commonly used in the nuclear power plants. However, no comments have been made on the damping of such perforated tubes because of limited observation till then. The general perception regarding damping is that the perforation in a structure increases damping. But not many experimental observations are available. The thrust of the present paper is again on the perforated structures, with focus in particular on the added of submerged strip/plate-type structures.

A series of modal experiments was conducted on laboratory-scale specimens (both perforated and non-perforated structures). These experiments were conducted on the test specimens for both submerged in water as well as non-submerged conditions. The results of the dynamic parameter study on perforated plates are presented in the paper. Based on experimental observations, a formulation for the estimation of added mass of submerged plate-type structures is attempted on a concept similar to the one given earlier for perforated tubes [6]. In addition, the damping behaviour of such perforated specimens with respect to non-perforated specimens of equivalent dimensions is also discussed based on experimental observations.

*Corresponding author. Tel.: +91-22-2559-1501; fax: +91-22-2550-5151.
E-mail address: vilred@magnum.barc.ernet.in (J.K. Sinha).

0022-460X/03/$ - see front matter
PII: S0022-460X(02)01023-4

2. Methodology for added mass estimation

Estimation of added mass has been done by modal experiment conducted on test specimens of different dimensions, supplemented by analysis. In the experimental part, the modal parameters—natural frequencies, mode shapes and damping were obtained for the perforated structures with and without submergence. The dynamic characteristics (natural frequencies and mode shapes) of the structural component without submergence would be totally dependent on the structural configurations (e.g., boundary conditions) and the material properties of the component. Whereas, the dynamic behaviour of the submerged structure would include the effect of fluid in addition to the parameters that determine the response of the non-submerged structure. Hence, in the analysis part, a mathematical model of the test specimen is constructed using finite element (FE) method. The FE model is simulated such that the computed eigenvalues and eigenvectors match closely with the experimental results of non-submerged case. Such a model would then be a true representation of the structure with actual boundary conditions as well as the material properties of the structure used. Using this FE model, the additional mass contribution by the surrounding fluid to the vibrating structures, i.e., added mass of fluid to the submerged specimen could be estimated so as to match the experimental results during submergence.

3. Test set-up and specimen

A schematic of the experimental test set-up is shown in Fig. 1(a). The set-up consists of a tank which houses the arrangement for the modal testing of test specimens mechanically clamped as cantilever. Test specimens of length 600 mm length with different thickness and width and perforation pattern were used for the study. The effective length of the specimen in the clamped condition was 550 mm. The test specimen of three different thickness—1, 2 and 3 mm and different width of 26.5 ± 1, 35.75 ± 0.5, 45.75 ± 0.25, 55.5 ± 0.5 and 83 ± 0.75 mm were used for study. A total of 36 test specimens (21 perforated and 15 non-perforated specimens of equivalent dimensions) made of aluminium were used for the study. Two types of perforation patterns of hole size 6.20 ± 0.25 mm were used for the study. Details of the perforated specimens with perforation patterns are shown in Fig. 2. Out of the 21 perforated specimens, 15 have perforation pattern as in Fig. 2(b) with 13 number of holes of size 6.20 ± 0.25 mm. Remaining six specimen have perforation pattern as shown in Fig. 2(c) with 39 holes (13 holes per row) each of hole size 6.20 ± 0.25 mm. The dimensions of the tank and the test specimens were chosen such that no wall effects have influence on the dynamics of the test specimens when the tank is filled with fluid (see Fig. 1(a)). The decision of choosing the tank dimensions was an engineering judgment totally based on the experimental observations by Chen [7] on the dynamics of a rod-shell system conveying fluid.

4. Experimental modal analysis

The modal parameters for all the test specimens were obtained by conducting impulse–response test [1]. This experiment was conducted on both perforated and non-perforated specimens of

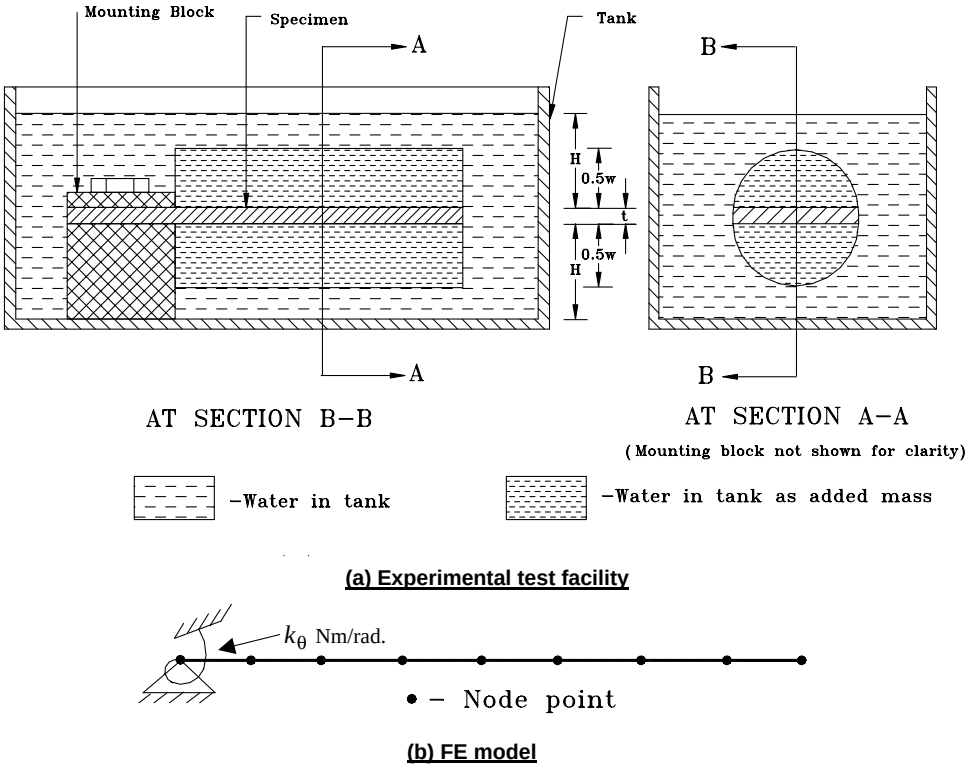

Fig. 1. Experimental test facility and the test specimen FE model.

equivalent dimensions in both submerged as well as non-submerged conditions. A small-instrumented hammer was used for the excitation of the specimen. The force sensor (PCB 208A02) of the hammer and tiny accelerometers (Entran PS-30A-2) were used for measurement of the exciting force and response of the specimen, respectively. Impulse was given near the clamped location and response was obtained using accelerometers from a few locations along the length. A 2-channel A & D 3525 FFT analyzer was used for the force and the acceleration data acquisition. Total four accelerometers were used on the centreline along the length of specimen at a distance of 130, 290, 410 and 550 mm from the clamped end. Depending upon the dimensions of the test specimens the frequency bandwidth and signal processing windows for the measured force and the responses were adjusted during modal tests. However, the 1600 frequency lines were always used for the modal tests. The measured time domain data were initially processed through the FFT analyzer to obtain the averaged frequency response functions (FRFs). Few typical FRFs (inertance) for the test specimen of width 35 and 3 mm thick are shown in Fig. 3. As can be seen from Fig. 3(a) the first three beam bending frequencies are well defined in the FRF for non-submerged conditions. However, for submerged case the first bending frequency is not well defined in the FRF shown in Fig. 3(b) for submerged case. The modal tests were repeated for the cases like this by reducing the frequency band to increase the frequency resolution so that the

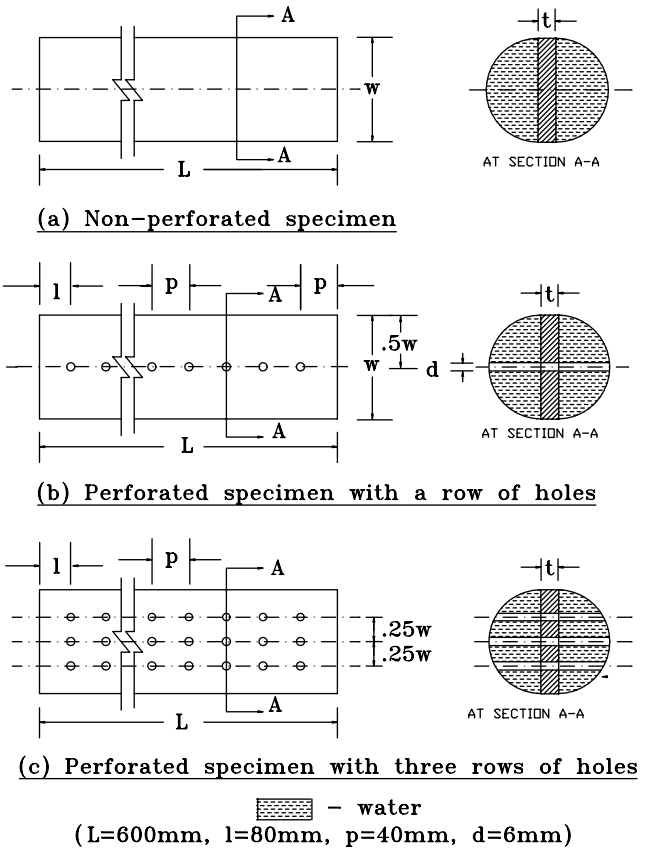

Fig. 2. Different test specimens used in the study.

lower modes could be identified confidently. Fig. 3(c) shows such example where first mode is well defined. The modal parameters, i.e., natural frequencies and modal damping were then extracted using single-degree-of-freedom (SDOF) curve fit on the experimental FRFs through computational program. Only the first few cantilever-beam-type modes were measured. The identified natural frequencies for perforated specimens are listed in Tables 1–3.

5. FE modelling and simulation

A mathematical model for the cantilever-type test specimen was made using FE method [8]. The FE model has been made using two noded Euler–Bernoulli beam elements (two-degree-of-freedom at each node, i.e., bending displacement and bending rotation) to simulate the cantilever-beam-type modes of the plate-type test specimens. Since, one end of the test specimens were clamped mechanically in the experimental test facility, the test specimens will have zero bending displacement at clamped location but may have a small rotation at that location. A spring element

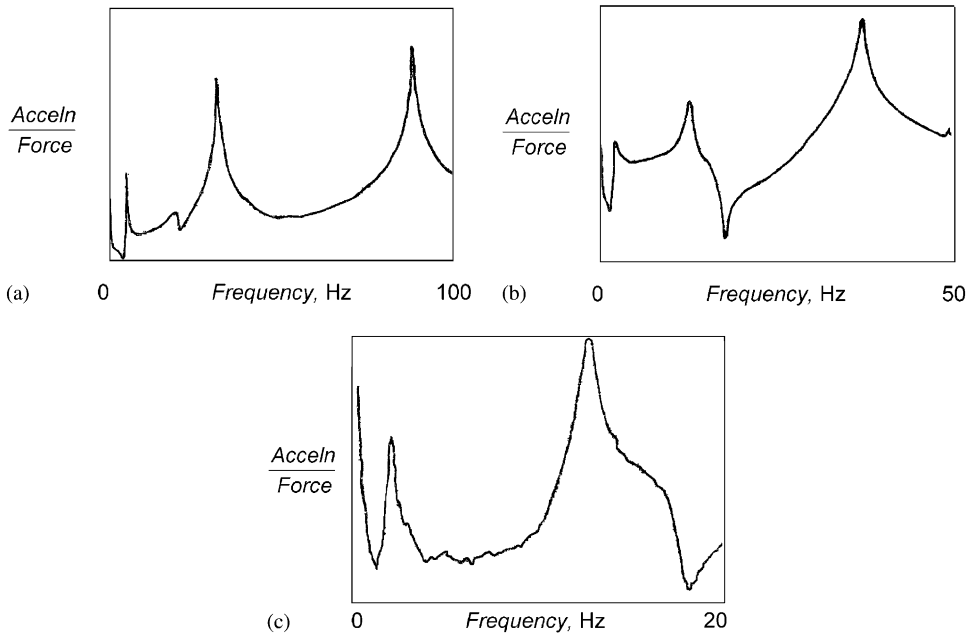

Fig. 3. Measured FRFs for the plate of 35 mm width and 3 mm thickness: (a) non-submerged condition, (b) submerged condition, and (c) submerged condition with reduced frequency bandwidth.

(SDOF at each node) for the rotational restraint at the clamped location was provided in the FE model to simulate expected small rotation at the clamped location. A typical FE model is shown in Fig. 1(b). To account for the inertial and stiffness effects due to the number of holes distributed all over in the perforated specimens, thickness equivalent to the volume of holes was removed uniformly from the thickness of the test specimens in the each element of the FE model. The mass of each accelerometer is only 3 g and its effect on the dynamics of the plates is expected to be insignificant. However, to avoid any possible error in the FE modelling the masses of the accelerometers were also included in the model.

Since the geometrical and the material properties were known for all the test specimens, the value of rotational boundary spring stiffness (k_θ Nm/rad) provided in the FE model was tuned so that the computed results match fairly well with the experimental results of non-submerged specimens. This rotational boundary spring stiffness will be different for different test specimens. The gradient-based sensitivity method for model updating [9–10] was used for the estimation of this rotational stiffness for each specimen. The updated FE model ensures that the entire structural features of the experimental set-up are fully reflected in the model. The computed natural frequencies for all the perforated specimens are also listed in Tables 1–3. It can be seen from the tables that the analytical results compare well with experimental ones.

To this FE model, the additional mass accounting for the surrounding water has to be added for the submerged condition of the specimen. The use of consistent mass for this added mass of the water may be better choice. However, for the low-frequency vibration the model with lumped

Table 1
Natural frequencies of perforated specimens of 1 mm thickness

Specimen details	Non-submerged			Submerged					
	Experimental freq. (Hz)	FE model freq. (Hz)	% Error	Experimental freq. (Hz)	FE model freq. Hz	% Error	Added mass		
							Experimental	Theoretical	% Error
$w = 25.66$ mm,	2.156	2.095	−2.83	0.875	0.800	−8.57			
$n = 13$	13.031	13.592	+4.30	4.925	5.027	+2.07	0.268	0.274	−2.189
	36.625	38.985	+6.44	14.099	14.086	−0.09			
$w = 35.25$ mm,	2.281	2.232	−2.15	—	0.728	—			
$n = 13$	14.156	14.340	+1.30	4.375	4.528	+3.49	0.527	0.521	+1.151
	40.313	40.839	+1.30	12.719	12.596	−0.97			
$w = 46.00$ mm,	2.406	2.400	−0.25	—	0.670	—			
$n = 13$	14.719	15.168	+3.05	4.150	4.182	+0.77	0.898	0.895	+0.335
	41.406	42.759	+3.26	11.888	11.665	−1.87			
$w = 55.00$ mm,	2.250	2.237	−0.58	—	0.577	—			
$n = 13$	14.250	14.259	+0.06	3.688	3.620	−1.84	1.273	1.282	−0.702
	40.250	40.457	+0.51	10.844	10.127	−6.61			
$w = 83.50$ mm,	2.650	2.531	−4.49	—	0.532	—			
$n = 13$	15.906	15.839	−0.42	3.475	3.311	−4.72	2.874	2.977	−3.460
	43.813	44.313	+1.14	10.075	9.216	−8.53			
$w = 55.00$ mm,	2.688	2.444	−9.07	—	0.618	—			
$n = 39$	14.938	15.371	+2.90	4.188	3.845	−8.21	1.277	1.254	+1.435
	41.969	43.177	+2.88	10.781	10.704	−0.71			
$w = 83.50$ mm,	2.529	2.369	−6.33	—	0.496	—			
$n = 39$	14.988	14.952	+0.24	3.650	3.117	−14.60	2.767	2.920	−5.240
	42.094	42.091	+0.00	10.600	8.733	−17.61			

'—' indicates frequency not identified.Table 1
Natural frequencies of perforated specimens of 1 mm thickness

Specimen details	Non-submerged	Submerged

Table 2
Natural frequencies of perforated specimens of 2 mm thickness

Specimen details	Non-submerged			Submerged					
	Experimental freq. (Hz)	FE model freq. (Hz)	% Error	Experimental freq. (Hz)	FE model freq. (Hz)	% Error	Added mass		
							Experimental	Theoretical	% Error
$w = 27.43$ mm,	4.875	4.935	+1.23	2.262	2.315	+2.34			
$n = 13$	30.688	31.039	+1.14	14.000	14.428	+3.05	0.311	0.314	−0.95
	87.125	87.185	+0.06	40.250	40.205	−0.11			
$w = 36.25$ mm,	4.938	5.007	+1.39	2.0938	2.074	−0.94			
$n = 13$	31.050	31.391	+1.09	12.594	12.923	+2.61	0.545	0.554	−1.60
	88.188	87.949	−0.27	36.938	36.007	−2.52			
$w = 45.63$ mm,	5.000	5.056	+1.12	1.938	1.906	−1.65			
$n = 13$	31.938	31.641	−0.92	11.438	11.878	+3.84	0.840	0.880	−4.50
	88.563	88.525	−0.04	34.344	33.099	−3.62			
$w = 55.93$ mm,	5.000	5.000	0.00	1.737	1.721	−0.92			
$n = 13$	31.875	31.331	−1.70	10.875	10.753	−1.12	1.251	1.327	−5.70
	87.750	87.723	−0.03	31.563	30.017	−4.89			
$w = 82.25$ mm,	4.938	5.095	+3.17	1.487	1.480	−0.47			
$n = 13$	31.938	31.869	−0.21	9.531	9.244	−3.01	2.636	2.892	−9.71
	89.375	89.090	−0.31	28.188	25.795	−8.48			
$w = 55.93$ mm,	5.125	5.055	−1.36	1.844	1.743	−5.47			
$n = 39$	31.750	31.577	−0.54	11.250	10.850	−3.55	1.216	1.284	−5.29
	89.188	88.196	−1.11	35.375	30.205	−14.61			
$w = 82.25$ mm,	4.938	5.130	+3.88	1.575	1.457	−7.49			
$n = 39$	31.813	32.012	+0.62	10.281	9.074	−11.74	2.725	2.831	−3.74
	89.625	89.321	−0.33	29.844	25.271	−15.32			

Table 2
Natural frequencies of perforated specimens of 2 mm thickness

Table 3
Natural frequencies of perforated specimens of 3 mm thickness

Specimen details	Non-submerged			Submerged!					
	Experimental freq. (Hz)	FE model freq. (Hz)	% Error	Experimental freq. (Hz)	FE model freq. (Hz)	% Error	Added mass		
							Experimental	Theoretical	% Error
$w = 25.59$ mm,	7.500	7.882	+5.09	4.188	4.213	+0.59			
$n = 13$	48.250	48.985	+1.52	26.563	26.184	−1.42	0.268	0.272	−1.47
	136.000	136.090	+0.06	76.625	72.746	−5.06			
$w = 35.25$ mm,	8.000	8.198	+2.47	3.938	3.980	+1.06			
$n = 13$	51.000	50.810	−0.37	24.438	24.223	−0.87	0.507	0.520	−2.50
	140.625	140.860	+0.16	70.563	67.151	−4.83			
$w = 45.87$ mm,	7.750	8.238	+6.29	3.500	3.539	+1.11			
$n = 13$	52.250	51.414	−1.60	21.250	22.040	+3.71	0.878	0.865	+1.50
	145.500	143.500	−1.37	68.125	61.371	−9.91			
$w = 55.50$ mm,	7.750	8.230	+6.19	3.375	3.253	−3.61			
$n = 13$	50.500	51.020	+1.02	21.125	20.167	−4.53	1.276	1.309	−2.52
	141.500	141.450	−0.03	63.125	55.914	−11.42			
$w = 83.63$ mm,	7.750	7.836	+1.10	2.650	2.680	+1.13			
$n = 13$	51.875	49.138	−5.27	19.750	16.795	−14.96	2.699	2.931	−7.91
	145.250	137.590	−5.27	55.875	46.983	−15.91			
$w = 55.50$ mm,	7.500	7.939	+5.85	3.438	3.285	−4.45			
$n = 39$	51.250	49.518	−3.37	22.313	20.454	−8.33	1.138	1.249	−8.88
	142.375	138.129	−2.98	66.563	56.949	−14.44			
$w = 83.63$ mm,	7.750	7.936	+2.40	2.875	2.645	+8.00			
$n = 39$	51.500	49.421	−4.03	20.813	16.474	−20.84	2.771	2.956	−6.25
	144.750	137.590	−4.94	56.688	45.862	−19.09			

Table 3
Natural frequencies of perforated specimens of 3 mm thickness

mass will also give sufficiently accurate results. So the lumped mass is used here. Hence, the lumped mass accounting for the surrounding water at the nodes of the specimen was increased till the natural frequencies match with the experimental values under submerged condition. The computed natural frequencies of the test specimens in water are also listed in Tables 1–3. Tables also list the experimentally estimated mass of the surrounding water to be added to the submerged specimens using FE analysis. Based on the above observations a formulation for added mass is attempted below.

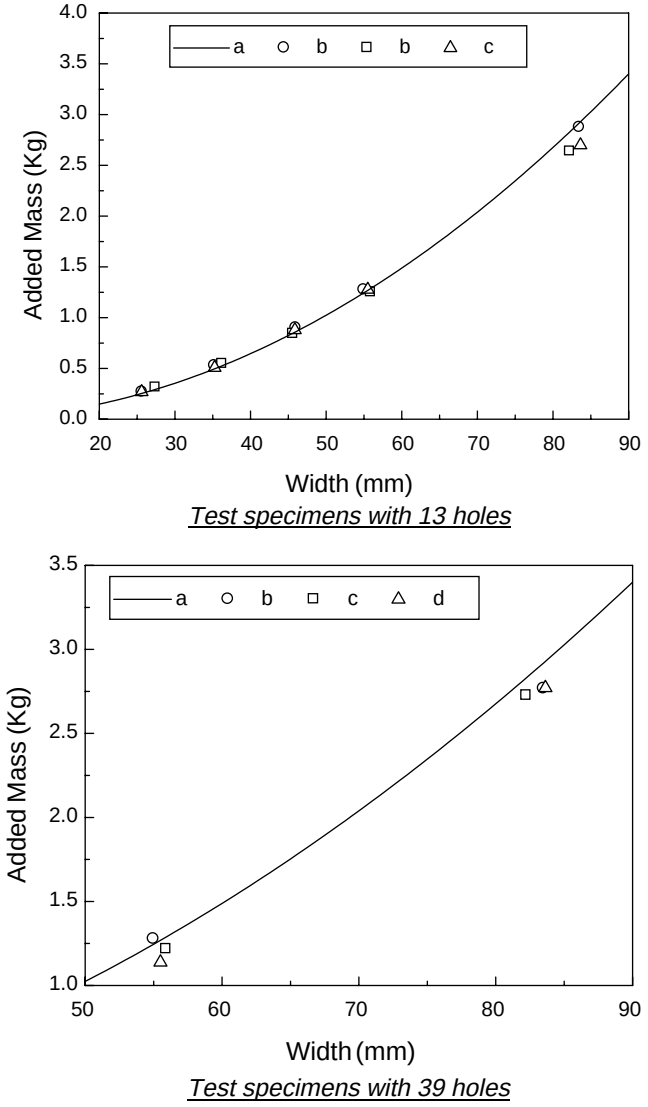

Fig. 4. Added mass of submerged perforated plate specimens (a: theoretical; b, c and d: experimental for 1 mm, 2 mm and 3 mm thick plate specimens, respectively).

6. Formulation for added mass

The added mass of the submerged vibrating object accounting for the surrounding fluid would be the mass of the fluid equivalent to the reaction force experienced by that object. Ideally for the example under discussion, the mass of fluid required to be added is the mass of fluid contained in an imaginary cylinder of diameter equal to plate width and length same as that of the plate [3]. The distribution of the reaction mass on either surface of the plate all along the length in the direction of vibration is represented in Fig. 2(a), neglecting the shear reaction along the thickness. This was observed for the submerged non-perforated specimens. However, for perforated specimens of equivalent dimensions, the added mass to be accelerated during vibration is smaller. The obvious reason is that the perforation in the structure is not accelerating some quantity of fluid, thus reducing the inertia in the transverse direction. The quantification for such a reduction is useful when one has to estimate the natural frequencies of such a perforated structure.

For non-perforated strip/plate-type structure, added mass accounting from the surrounding fluid (as from [3, p. 25]) is given as

$$M_{nf} = \frac{\pi}{4} w^2 L \rho_f,$$

where L is the length of the plate, w the width of the plate and ρ_f the density of the surrounding fluid.

Whereas for perforated plate-type structure, added mass accounting for the surrounding fluid based on a similar concept given earlier by Sinha and Moorthy [6] can be defined as

$$M_{pf} = \frac{\pi}{4} w^2 L \rho_f - M_h,$$

where M_h is the mass of fluid that does not accelerate and is equal to the fluid mass contained in the total volume of imaginary cylinders formed by the holes (see pictorial representation in Fig. 2(b) and (c)); $M_h = \sum_{i=1}^{n} A_i L_i \rho_f$, $i = 1, 2, \ldots, n$, A_i is the cross-sectional area of ith hole in the vibratory plane; $A_i = (\pi/4) d_i^2$, L_i the chord length of the imaginary cylinder at ith hole location; d_i the diameter of ith hole and n the total number of holes in the perforated structure.

The above formulation of added mass could be useful for the perforated plate-type structures submerged in stationary, incompressible and inviscid fluid. It may also be noted that if the perforation in the plate is uniformly distributed over the entire surface area of the plate then the mass of fluid lumped to the nodes of FE model would also be uniform. It was the case for the perforated specimens used for the study. However, in many cases the distribution of perforation

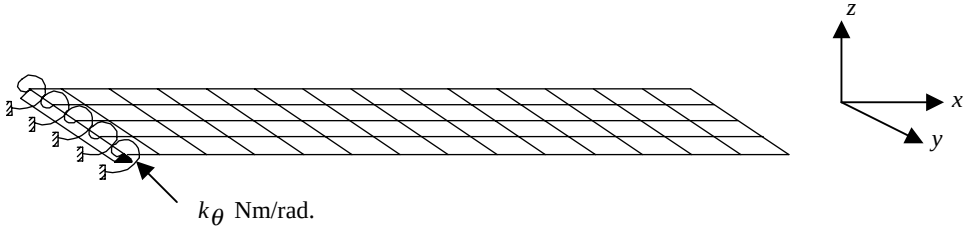

Fig. 5. Typical FE model using plate elements.

Table 4
Natural frequencies of perforated specimens of 83 mm width

Specimen details	Non-submerged			Submerged		
	Experimental freq. (Hz)	FE model freq. (Hz)	% Error	Experimental freq. (Hz)	FE model freq. (Hz)	% Error
$w = 83.50$ mm,	2.650	2.474	−6.64	—	0.514	—
$t = 1$ mm, $n = 13$	15.906	15.914	+0.05	3.475	3.279	−5.64
	—	35.221	—	—	8.852	—
	43.813	46.160	+5.35	10.075	9.385	−6.84
$w = 83.50$ mm,	2.529	2.337	−7.59	—	0.499	—
$t = 1$ mm, $n = 39$	14.988	15.223	+1.56	3.650	3.196	−12.43
	—	34.474	—	—	8.713	—
	42.094	44.462	+5.62	10.600	9.171	−13.48
$w = 82.25$ mm,	4.938	4.973	+0.70	1.487	1.446	−2.75
$t = 2$ mm, $n = 13$	31.938	31.950	+0.03	9.531	9.165	−3.84
	—	71.467	—	—	24.503	—
	89.375	92.581	+3.58	28.188	26.138	−7.27
$w = 82.25$ mm,	4.938	4.981	+0.87	1.575	1.441	−8.50
$t = 2$ mm, $n = 39$	31.813	31.852	+0.12	10.281	9.180	−10.70
	—	70.252	—	—	24.806	—
	89.625	92.019	+2.67	29.844	26.266	−11.98
$w = 83.63$ mm,	7.750	8.010	+13.33	2.650	2.764	+4.30
$t = 3$ mm, $n = 13$	51.875	50.827	−2.02	19.750	17.387	−11.96
	—	106.497	—	—	43.678	—
	145.250	146.041	+0.54	55.875	49.295	−11.77
$w = 83.63$ mm,	7.750	7.966	+2.78	2.875	2.754	−4.20
$t = 3$ mm, $n = 39$	51.500	50.507	−1.92	20.813	17.303	−16.86
	—	104.950	—	—	43.185	—
	144.750	145.050	+0.20	56.688	49.021	−13.52

Remarks: Mode 1: First cantilever beam mode of plates. Mode 2: Second cantilever beam mode of plates. Mode 3: First wrapping mode of plates about its axis along the length. Mode 4: Third cantilever beam mode of plates. Mode shapes shown in Fig. 6.Table 4
Natural frequencies of perforated specimens of 83 mm width

(both pitches and hole sizes) varies along the length. This has to be taken care while calculating the additional lumped mass of surrounding fluid to be added to the nodes of FE model.

For all the elucidated examples, the theoretically estimated added mass using the above-suggested formula is also listed in Tables 1–3 along with the experimentally estimated added mass using FE analysis. Fig. 4 is the graphical representation of the variation of theoretical added mass (suggested formula) with increasing width of perforated plate having 13 holes and 39 holes. Experimental added mass is also shown in Fig. 4. As can be seen from the tables, the error between the two estimates for all examples is small and well within $\pm 9\%$. The change in the natural frequencies due to this order of the error in the estimation of mass is expected to be small.

The computed natural frequencies (see Tables 1–3) are also within $\pm 6\%$ except for few cases where error is of the order 8–21% mainly for specimens of higher width. This order of error was also observed in frequency estimation for the non-perforated specimens of equivalent dimensions.

One possible reason for high error seen in the computed frequencies could be the FE modelling of plate-type specimens of higher width as beam elements. Hence, the specimens with 83 mm width were modelled again using plate elements. Total 56 plate elements were used in modelling. The clamped end of the specimen was modelled as earlier, i.e., the rotational springs at the clamped end to allow some rotation in the test specimen. A typical FE model is shown in Fig. 5. Once again the value of the spring was estimated using the experimental modal data for non-submerged condition by the gradient-based sensitivity model updating method [9–10]. To this updated FE model the added mass of water calculated using the suggested formula was distributed as per the cylindrical fluid reaction profile shown in Figs. 1 and 2 to the nodes of the FE model. The improvement in the FE predictions can be seen from Table 4. Typical mode shapes both experimental and analytical are also shown in Fig. 6. The analytically computed wrapping mode of the plates was not identified in the modal experiments as the measurements were on the centreline along the length. However, the significant improvements in the computed natural frequencies have been noticed when plate elements used for the FE modelling compared to the model using beam elements. The error in the computed natural frequencies is now smaller than

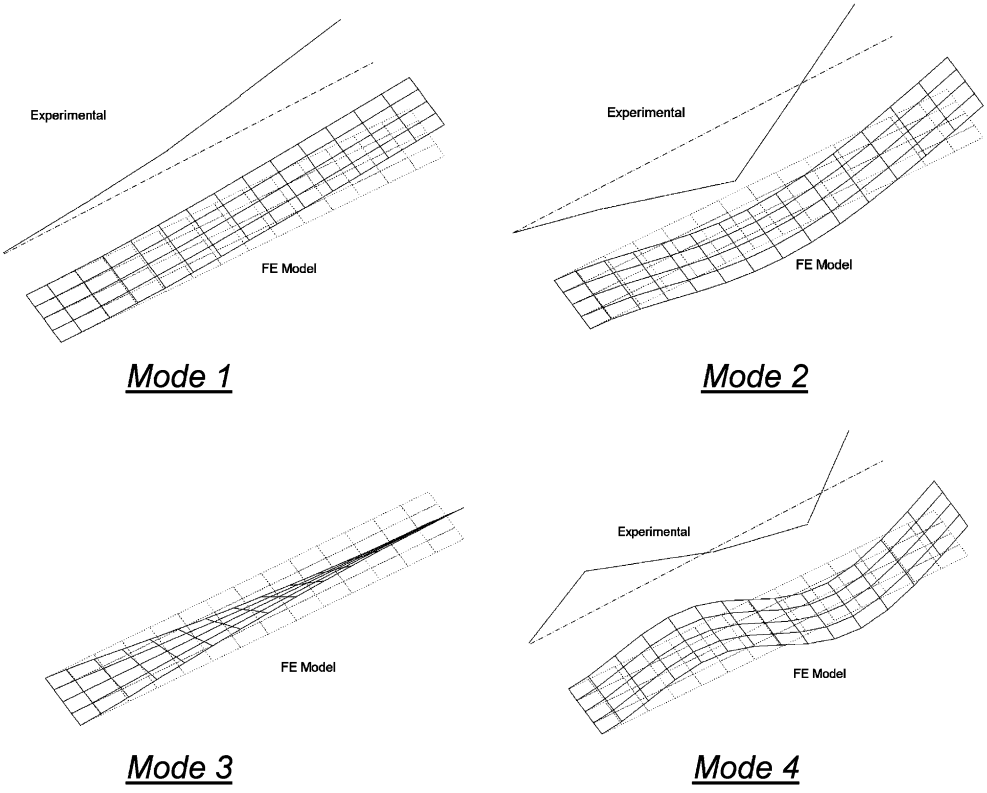

Fig. 6. Experimental and analytical mode shapes.

the earlier with zero error between the experimental and analytical added mass. Thus, the suggested formula for estimation for *added mass* for the submerged perforated plate-type structure could be deemed as fairly accurate and could be useful at design stage.

7. Damping

As brought out in Section 3, the modal damping was also extracted using SDOF curve fitting on the experimental FRFs for both perforated and non-perforated specimens. The values of damping ratio (%) are shown graphically for first three modes in Figs. 7–9 for perforated specimens. The corresponding non-perforated specimens of equivalent dimensions are also shown in the figures for easy comparison. As can be seen from the figures the damping values have wide scatter to establish any formulation for the damping estimation for the perforated plates. The manual uncontrolled impulse given during modal tests could be the possible reason for the scatter seen in the damping values though best effort was made to give same excitation level during the

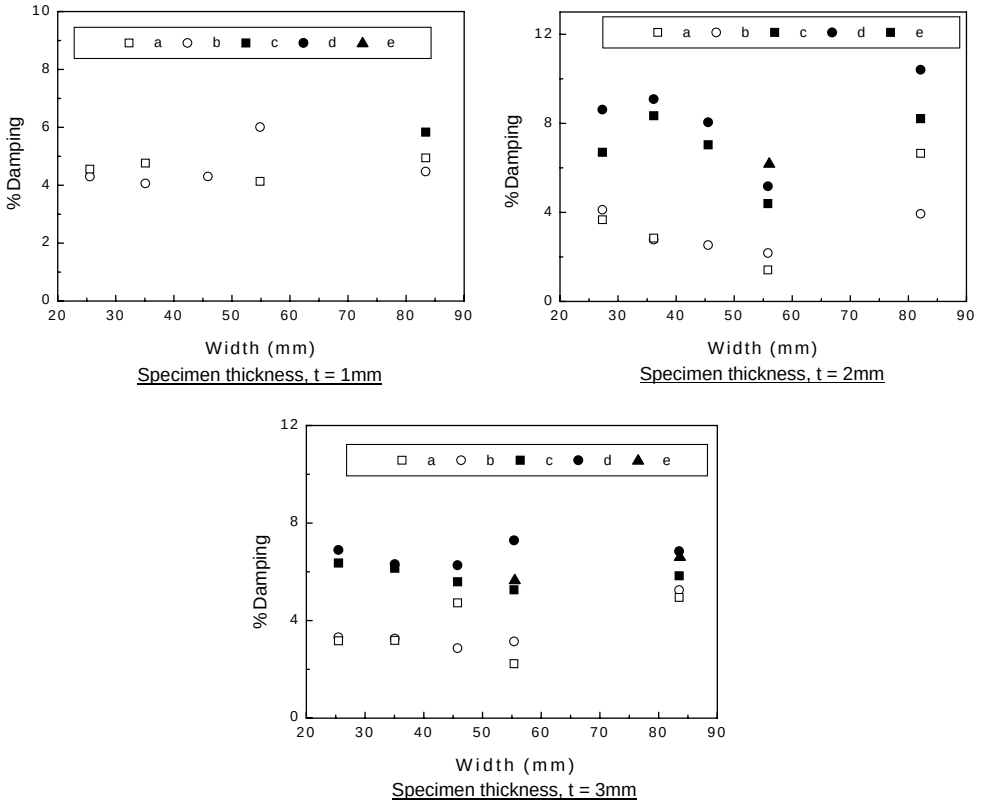

Fig. 7. Damping at first mode of test specimens: (a) non-submerged non-perforated, (b) non-submerged perforated with13 holes, (c) submerged non-perforated, (d) submerged perforated with 13 holes, and (e) submerged perforated with 39 holes.

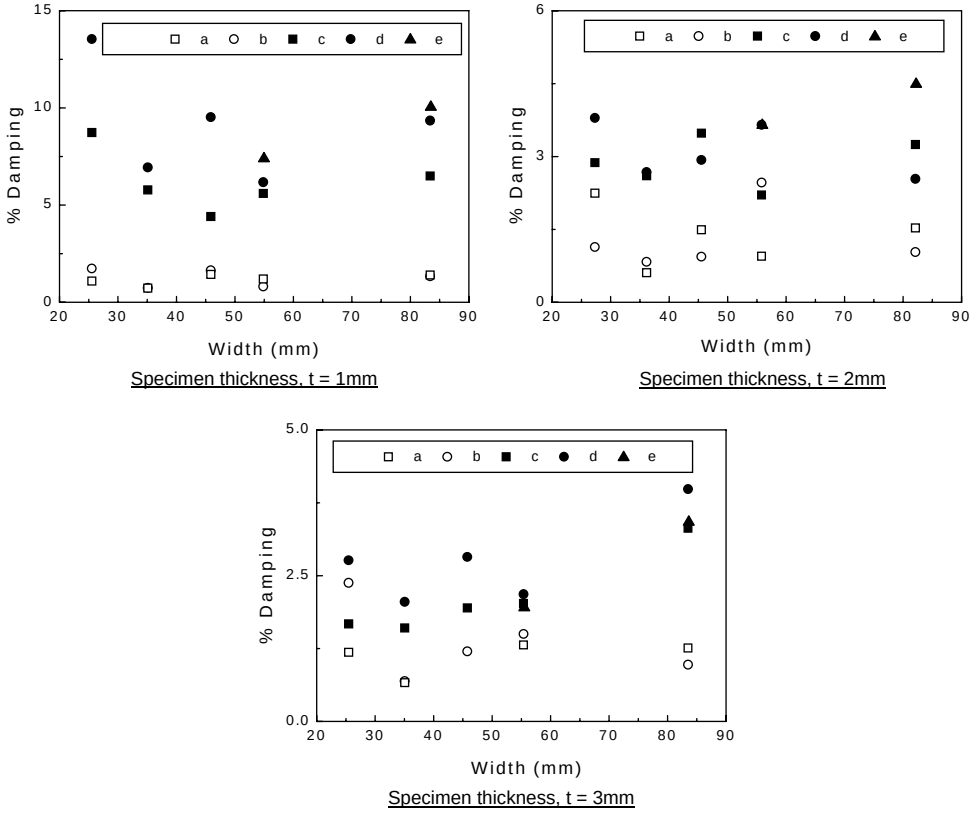

Fig. 8. Damping at second mode of test specimens: (a) non-submerged non-perforated, (b) non-submerged perforated with13 holes, (c) submerged non-perforated, (d) submerged perforated with 13 holes, and (e) submerged perforated with 39 holes.

modal tests for all specimens. Even with these scattered damping values some trends seem to be emerging out, as discussed here.

Damping ratio for perforated plates decreases from first to third mode for both submerged and non-submerged conditions. This is consistent with earlier observations made by Moorthy and Sinha [11] on perforated tubes. Damping for higher modes was not measured. In general, no significant difference between the damping of perforated and non-perforated specimens in non-submerged condition was observed. However, damping is significantly high in submerged condition for perforated structures for many cases compared to non-perforated ones. Some trends of increase in damping with increase in number of holes were also observed. The controlled step-sine excitation for all specimens will explore these features clearly. Such an experiments is underway.

Few earlier studies [6,11–12] on perforated structures (perforated tubes) have also given the experimental damping values, but none of them have compared these values with the experimental damping values for non-perforated tubes of equivalent dimensions. Hence, the observation of the increase in damping due to perforation may be considered as a useful piece of information in the

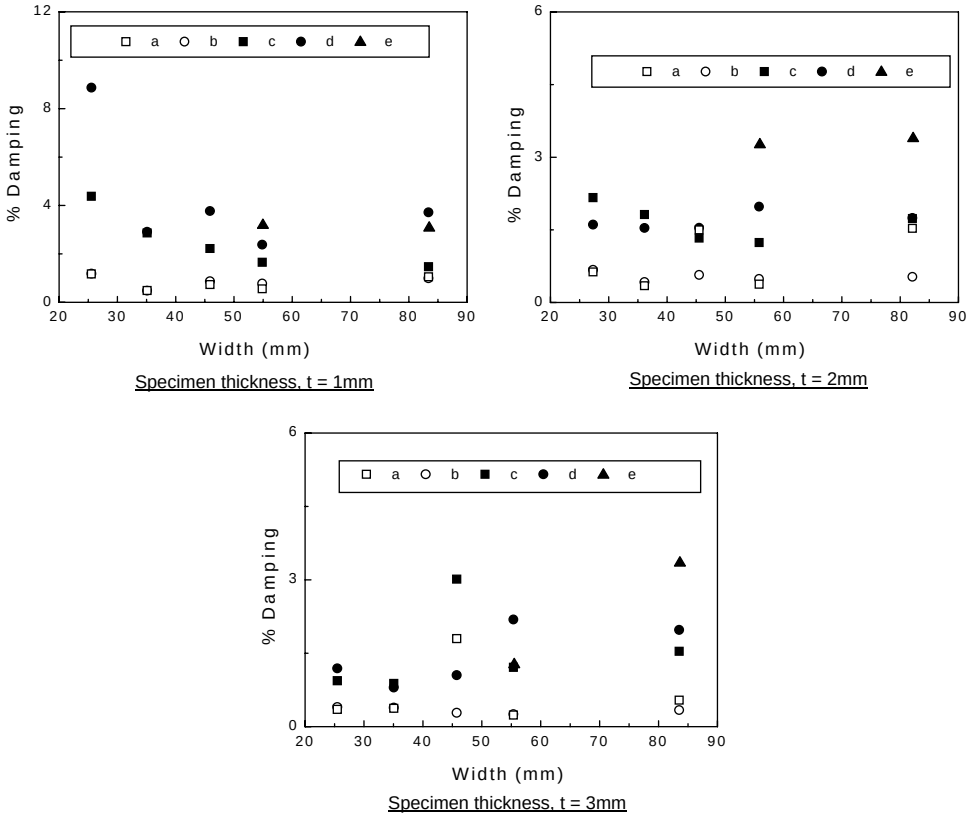

Fig. 9. Damping at third mode of test specimens: (a) non-submerged non-perforated, (b) non-submerged perforated with13 holes, (c) submerged non-perforated, (d) submerged perforated with 13 holes, and (e) submerged perforated with 39 holes.

domain of structural dynamics as no such comparative study has been reported earlier to the knowledge of authors.

8. Conclusion

Based on the experimental and analytical studies on a number of test specimens, a formula is being suggested for added mass of the vibrating perforated plate-type structures submerged in fluid. This could be of considerable importance to designers for structural dynamic evaluation of such components without the need to conduct a modal test.

Damping is another important parameter for complete dynamic characterization and design evaluation of structures under dynamic loading. It was observed that the damping of the submerged perforated structures is generally higher compared to submerged non-perforated structures of equivalent dimensions. The trend of increase in the damping with the number of holes in the submerged perforated structures is also observed for most cases. However, the effect

of size of the holes on damping could not be studied. The formulation for estimation of damping could also not be possible. This requires further study on a number of perforated structures with different number of holes, hole sizes, pitches, etc. Such a study is underway.

Acknowledgements

Authors acknowledge the motivation and consistent support provided by Mr. R.K. Sinha, Associate Director, Reactor Design and Development Group, BARC, Mumbai-400 085 in carrying out this work. The auxiliary support by Mr. Satyavir Singh, SA/C, Vibration Laboratory, R.E.D., BARC for the fabrication of the test specimens and the experimental test set-up is also acknowledged.

References

[1] D.J. Ewins, Modal testing—Theory and Practice, Research Studies Press, Taunton, UK, 1984.
[2] S.S. Chen, Flow-Induced Vibration of Circular Cylindrical Structures, Hemisphere, New York, 1987.
[3] R.D. Blevins, Flow Induced Vibration, 2nd edition, Van Nostrand Reinhold, New York, 1990.
[4] R.D. Blevins, Formulas for Natural Frequency and Mode Shape, Van Nostrand Reinhold, New York, 1979.
[5] E. Naudascher, R. Donald, Flow-Induced Vibration: An Engineering Guide, A.A. Balkema, Rotterdam, 1994.
[6] J.K. Sinha, R.I.K. Moorthy, Added mass of submerged perforated tubes, Nuclear Engineering and Design 193 (1999) 23–31.
[7] S.S. Chen, Dynamic of a rod-shell system conveying fluid, Nuclear Engineering and Design 35 (1974) 223–233.
[8] R.D. Cook, D.S. Malkus, M.E. Plesha, Concept and Applications of Finite Element Analysis, Wiley, New York, 1989.
[9] M.I. Friswell, J.E. Mottershead, Finite Element Model Updating in Structural Dynamics, Kluwer Academic Publishers, Dordrecht, 1995.
[10] J.K. Sinha, M.I. Friswell, Model updating: a tool for reliable modelling, Design Modification and Diagnosis, Shock Vibration Digest 34 (2002) 27–35.
[11] R.I.K. Moorthy, J.K. Sinha, Dynamic qualification of complex structural components of nuclear power plants, Nuclear Engineering and Design 180 (1998) 147–154.
[12] K. Muto, K.K. Kuroda, Y. Kasai, Forced vibration test of 1/5 scale model of CANDU Core, Proceedings of Fifth International Conference on Structural Mechanics in Reactor Technology, Vols. 12/3, Berlin, Germany, August 13–17, 1979.